ADVANCED ENERGY MATERIALS
www.advenergymat.de

A Novel Oligomer as a Hole Transporting Material for Efficient Perovskite Solar Cells

Peng Qin, Nicolas Tetreault, M. Ibrahim Dar, Peng Gao, Keri L. McCall, Simon R. Rutter, Simon D. Ogier, Neil D. Forrest, James S. Bissett, Michael J. Simms, Aaron J. Page, Raymond Fisher, Michael Grätzel, and Mohammad Khaja Nazeeruddin**

Among the third generation low cost PV devices, dye sensitized solar cells (DSSC) are front runners in converting solar energy into electricity, due to their low cost and ease of fabrication.[1,2] In DSSCs, the device architecture comprised of nanostructured TiO_2 as an electron conductor, a sensitizer as a light absorber, a redox mediator for dye regeneration and a counter electrode to collect electrons from the circuit and regenerate the redox mediator. Currently DSSCs exhibit >12.0% power conversion efficiency (PCE)[3] on the laboratory scale and ≈10% in a module.[4] The development of solid state DSSC (ss-DSSC), where liquid electrolyte was replaced by a solid hole conductor is an attracting option for commercial applications. Using 2,2′,7,7′-tetrakis(*N*,*N*-di-p-methoxyphenylamine)-9,9′-spirobifluorene (spiro-MeOTAD) as a solid hole transporting material (HTM), a power conversion efficiency of 7% has been achieved.[5] The efficiency was limited mainly due to the thin film configuration of TiO_2 layer and the lower molar extinction coefficient of sensitizers.

The hybrid organic-inorganic lead halide perovskites ($(RNH_3)PbX_3$, R = alkyl, X = Cl, Br, I), pioneered by Mitzi et al. have been recognized for their excellent semiconducting and light absorbing properties.[6,7] The ease with which these materials can be prepared and processed from solution have made them attractive for photovoltaic applications following the pioneering work of Miyasaka and co-workers.[8] In their studies, with methylammonium lead iodide perovskite as a light absorber and iodine/iodide as a redox electrolyte, a power conversion efficiency of 3.8% was obtained. Futher studies regarding the effect of titanium surface on perovskite processing were carried out by Park and co-workers, showing an improved efficieny of 6.5%.[9] The relatively low efficiency is mainly due to the solubility of the perovskite in the iodine/iodide based liquid electrolyte. High efficiencies have been realized by replacing the liquid electrolyte with solid hole transporting material, spiro-MeOTAD.[10,11] Interestingly, Lee et al. showed that a mixed lead halide perovskite on a mesoporous Al_2O_3 photoanode acts both as light absorber and electron conductor and obtained 10.9% efficiency.[11] The mesoporous Al_2O_3 acts as a mesoporous scaffold for a few nanometer of $CH_3NH_3PbI_2Cl$ deposition, and spiro-MeOTAD collects the holes and transports them to the back contact. Etgar et al. showed that the pure methylammonium lead iodide perovskite can also act as an efficient hole conductor,[12,13] demonstrating the interesting properties of these materials that they not only act as light absorbers but also participate in the electron and hole extraction. Later, Burschka et al. published a new record power conversion efficiency of over 15% where the perovskite has been deposited by a novel sequential deposition technique on mesoporous TiO_2 film.[14] Similar efficiencies were obtained by using a planar heterojunction architecture made by vapor deposition method,[15] and by using solution processible $ZnO/CH_3NH_3PbI_3$/spiro-MeOTAD structure.[16] Several groups have optimized perovskite solar cell efficiency by using various deposition conditions.[17–23]

In order to fabricate the solution-processed, stable, cost effective and high-efficiency solid-state solar cells, polymers were used as HTM instead of spiro-MeOTAD, including poly(3-hexylthiophene) (P3HT), poly-[2,1,3-benzothiadiazole-4,7-diyl[4,4-bis(2-ethylhexyl)-4H-cyclopenta[2,1-*b*:3,4-*b*′] dithiophene-2,6-diyl]] (PCPDTBT), (poly-[[9-(1-octylnonyl)-9H-carbazole-2,7-diyl]-2,5-thiophenediyl-2,1,3-benzothiadiazole-4,7-diyl-2,5-thiophenediyl]) (PCDTBT) and poly-triarylamine (PTAA).[24–27] It was shown that PTAA exhibits the best performance and provides the highest PCE (12.3%)[25] among the polymeric HTMs investigated, with higher open-circuit voltage (V_{oc}) and fill factor (*FF*) than spiro-MeOTAD under the same conditions.[24] Besides these polymers, the pyrene based small molecules[28] and inorganic HTMs[29,30] were also tested, showing maximum efficiencies of 12.4% in both cases.

Herein, we report on the use of a novel 2,4-dimethoxy-phenyl substituted triarylamine oligomer S197 (**Figure 1**) as HTM in $CH_3NH_3PbI_3$ based devices. Solar cells based on this new HTM

Dr. P. Qin, Dr. N. Tetreault, Dr. M. I. Dar, Dr. P. Gao, Prof. M. Grätzel, Prof. M. K. Nazeeruddin
Laboratory of Photonics and Interfaces
Institute of Chemical Sciences and Engineering
École Polytechnique Fédérale de Lausanne (EPFL)
Station 6 CH-1015, Lausanne, Switzerland
E-mail: michael.graetzel@epfl.ch;
mdkhaja.nazeeruddin@epfl.ch
Dr. K. L. McCall, Dr. S. R. Rutter, Dr. S. D. Ogier
Centre for Process Innovation Ltd, NETPark
Thomas Wright Way
Sedgefield, County Durham, TS21 3FG, UK
Dr. N. D. Forrest, Dr. J. S. Bissett, Dr. M. J. Simms, Dr. A. J. Page, Dr. R. Fisher
Peakdale Molecular Ltd., Peakdale Science Park
Sheffield Road, Chapel-en-le-Frith, High Peak, SK23 0PG, UK
Prof. M. K. Nazeeruddin
Center of Excellence for Advanced Materials Research (CEAMR)
King Abdulaziz University
Jeddah, Saudi Arabia

DOI: 10.1002/aenm.201400980

 © 2014 WILEY-VCH Verlag GmbH & Co. KGaA, Weinheim

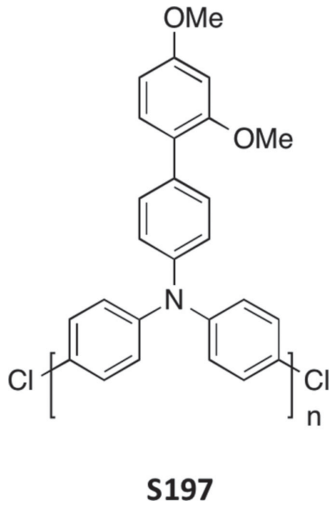

Figure 1. Chemical structure of oligomer S197.

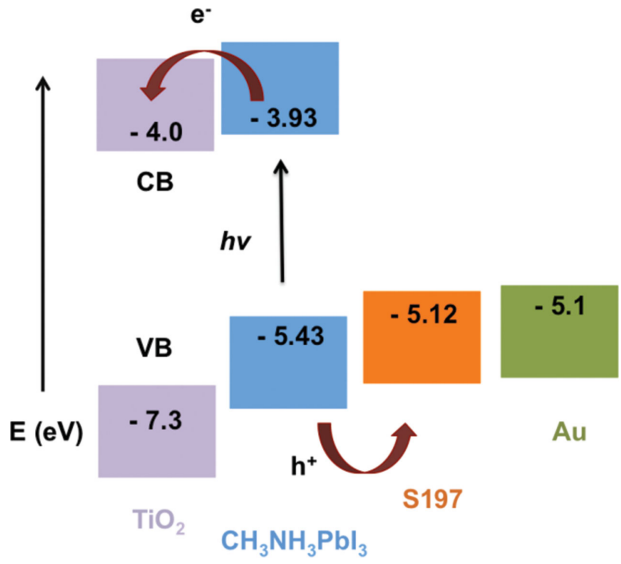

Figure 2. Energy level diagram of the $TiO_2/CH_3NH_3PbI_3$/S197/Au heterojunction solar cell.

showed a short-circuit current density (J_{sc}) of 17.6 mA cm^{-2}, V_{oc} of 967 mV, *FF* of 0.70, leading to a power conversion efficiency of 12.0% under 99.6 mW cm^{-2} illumination. To the best of authors knowledge, this is the first time that such an oligomer has been used in fabricating highly efficient $CH_3NH_3PbI_3$ based solar cells.

The S197 was prepared by the polymerization of *N*,*N*-bis(4-chlorophenyl)-2′,4′-dimethoxy-[1,1′-biphenyl]-4-amine, which was synthesized by the coupling reaction from 4-chloroaniline and 4-chloroiodobenzene. Triarylamine unit is used as the main chain due to the ease of oxidation, and its good charge carrier transport property, which has been widely applied in various electro-optical materials.[31] The optical and electrochemical properties of this poly-triarylamine are further modified by introducing the 2,4-dimethoxyphenyl group on the para position. The presence of Cl is mainly required for polymerization. In addition its effect on the electronic properties of the whole oligomer is to stabilize the highest occupied molecular orbital (HOMO) energy level. Detailed synthetic procedures can be found in the experimental section. The number average molecular weight (M_n) of the final product determined by gel permeation chromatography was found to be 3368 g mol^{-1}, with n = 8.8 and a polydispersity of 2.4.

The HOMO energy level of S197 determined by photoelectron spectroscopy was found to be 5.12 eV, which is higher than that of $CH_3NH_3PbI_3$, allowing efficient hole transfer from $CH_3NH_3PbI_3$ to S197, and subsequently through it to the Au counter electrode. As seen from the energy diagram in **Figure 2**, the energy levels of TiO_2, $CH_3NH_3PbI_3$, and S197 are well aligned which could allows efficient charge extraction.

The hole mobility of S197 was measured by using organic thin film transistors (OTFTs) with W/L = 15000/5 µm, (Figure S1, Supporting Information). This study showed a hole mobility of 5.1×10^{-4} cm^2 V^{-1} s^{-1} which is higher by an order of magnitude as compared with that of the most commonly used small molecule spiro-MeOTAD (M_w = 1225 g mol^{-1}, 4×10^{-5} cm^2 V^{-1} s^{-1}), but lower than high molecular weight polymer PTAA (M_w = 17500 g mol^{-1}, 4×10^{-3} cm^2 V^{-1} s^{-1}). Being significantly smaller than PTAA, the S197 can easily contact with the $CH_3NH_3PbI_3$.

The confluence of lower molecular weight with the appropriate hole mobility makes it a good HTM candidate for perovskite based photovoltaics.

In our devices, the perovskite films were prepared by first spin-coating of 1.0 M lead iodide (PbI_2) solution on the mesoporous TiO_2 films, followed by dip-coating of resulting TiO_2/PbI_2 films into a solution of methylammonium iodide (CH_3NH_3I). The dip-coating process resulted in an immediate change (5–10 s) in color of the film from light yellow to dark brown, indicating the formation of $CH_3NH_3PbI_3$.[14] We have investigated the effect of spin-speed used for PbI_2 deposition on the morphology of the final $CH_3NH_3PbI_3$ film by field emission scanning electron microscopy (FESEM). **Figure 3** shows the top-view of the films obtained at four different spin-speeds ranging from 5500 rpm to 8500 rpm. As it is evident that using a spin speed of 5500 rpm, a uniform overlayer of $CH_3NH_3PbI_3$ nanocrystals (Figure 3a) covering adequately underlying mesoporous TiO_2 was obtained compared to the films formed

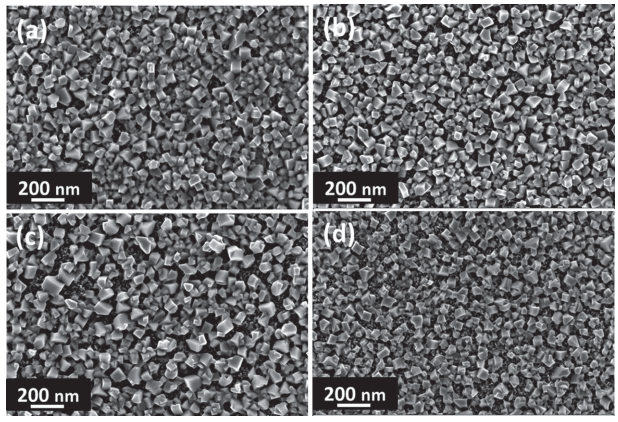

Figure 3. SEM images dispalying the top view of $CH_3NH_3PbI_3$ nanostructures obtained using different spin-speeds for PbI_2 deposition: a) 5500 rpm, b) 6500 rpm, c) 7500 rpm, and d) 8500 rpm.

© 2014 WILEY-VCH Verlag GmbH & Co. KGaA, Weinheim

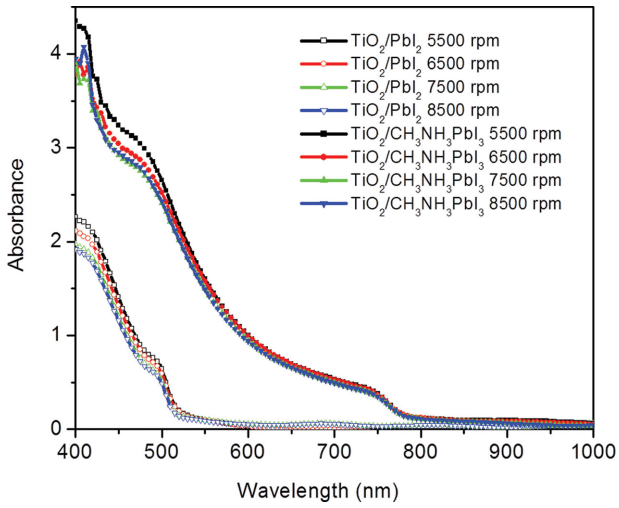

Figure 4. The absorbance spectra of TiO_2/PbI_2 and $TiO_2/CH_3NH_3PbI_3$ electrodes at different spin-speeds of PbI_2 deposition.

at higher spin-speeds. With higher spin-speeds, the perovskite appears to coat the TiO_2 partially, especially when it is over 8000 rpm. In addition to an expected loss in photocurrent, this would lead to direct contact between TiO_2 and HTM that would eventually bring down the fill factor and photovoltage.

To further investigate the perovskite loading on the mesoporous TiO_2 photoanode, UV–vis spectra were recorded of the TiO_2/PbI_2 films before and after converting to perovskite (**Figure 4**). The PbI_2 loading was found to decrease systematically with increasing spin-speed. After converting to perovskite, no significant difference in absorbance was observed between 520 nm to 800 nm while using different spin-speeds. However, in the lower wavelength region (below 500 nm), the sample with the slowest spin-speed (5500 rpm) showed unexpectedly higher absorption which could be attributed to the unconverted PbI_2 present in the sample. From the absoption studies, it could be surmarised that the PbI_2 can not be converted completely to $CH_3NH_3PbI_3$ under given conditions if the layer is quite dense and thick.

The HTM, S197, was subsequently deposited by spin-coating a solution of S197, 4-tert-butylpyridine (TBP) and lithium bis(trifluoromethylsulphonyl)imide (LiTFSI) in chlorobenzene onto the $TiO_2/CH_3NH_3PbI_3$ photoanode. Given its low molecular weight, it could readily penetrate into the remaining pore volume of the $TiO_2/CH_3NH_3PbI_3$ electrode. **Figure 5** shows the cross sectional SEM images of a device fabricated using a spin speed of 6500 rpm for PbI_2 deposition. The sequential deposition method leads to the formation of perovskite overlayer with homogeneos thinkness (Figure 5a) through out the dimension of the substrate. In addition to infilitrate among $CH_3NH_3PbI_3$ nanocrystals, as evident from high magnification SEM (Figure 5b), $a \approx 70$–100 nm S197 capping overlayer is formed ensuring proper electron blocking between the perovskite and the thermally evaporated gold (60 nm) counter electrode.

The current–voltage (J–V) properties were measured in dark and under illumination. **Figure 6** shows the J–V characteristics of the champion devices based on the structure: FTO/compact TiO_2/mesoporous $TiO_2/CH_3NH_3PbI_3$/S197/Au. The best photovoltaic performance with J_{sc} of 17.6 mA cm^{-2}, V_{oc} of 967 mV, *FF* of 0.70, and an overall PCE of 12.0% was obtained while using 6500 rpm spin-speed condition for PbI_2 deposition. **Table 1** shows the summary of the photovoltaic parameters of the best devices and the average of a selection of cells made under the same conditions. The statistical data are summarized in Table S1-S4 in the Supporting Information. It was found that the J_{sc} initially increases with the increase of PbI_2 deposition spin-speed until 6500 rpm, followed by a drop at higher spin-speed. Inspite of the fact that the device obtained using the slowest spin speed, i.e., 5500 rpm for PbI_2 deposition, displays the formation of the most uniform $CH_3NH_3PbI_3$ overlayer on the TiO_2 surface, the J_{sc} obtained was lower than that of a device obtained at 6500 rpm. Such a diminution in the J_{sc} could be attributed to the presence of unconverted PbI_2 as established from absoption studies. Further enhancement in the spin-speed leads to the formation of non-uniform $CH_3NH_3PbI_3$ film and such an improper coverage could enhance the contact between TiO_2 and S197, therefore the recombination between the electrons and holes. In summary, a spin-speed of 6500 rpm was found to be optimum for obtaining a device with better conversion of PbI_2 to $CH_3NH_3PbI_3$ and relatively the best loading. The incident-photon-to-current conversion efficiency (IPCE) for the best device with 12.0% *PCE* is shown in Figure S2 (Supporting Information), with a photocurrent response from 400 nm to 800 nm. The integration of IPCE spectrum showed a current density of 18.1 mA cm^{-2}, which is in agreement with the current density measured from I–V curve.

The high molecular weight polymer PTAA (M_w = 17500 g mol^{-1}) was also tested under similar conditions for comparison. The best device with PTAA exhibited J_{sc} of

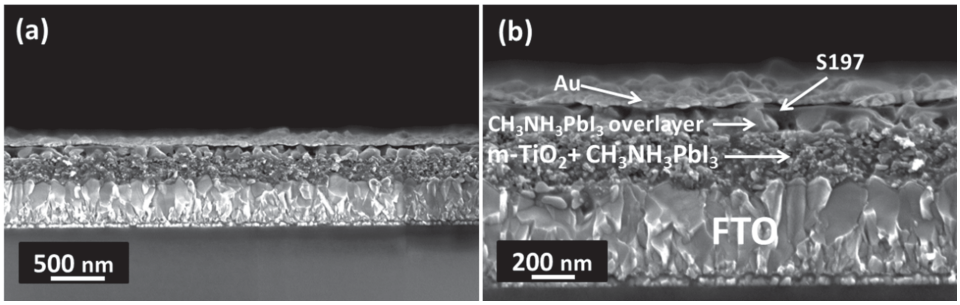

Figure 5. Cross-sectional SEM images of the device with 6500 rpm PbI_2 deposition at a) low magnification and b) high magnification.

© 2014 WILEY-VCH Verlag GmbH & Co. KGaA, Weinheim

ADVANCED ENERGY MATERIALS
www.advenergymat.de

www.MaterialsViews.com

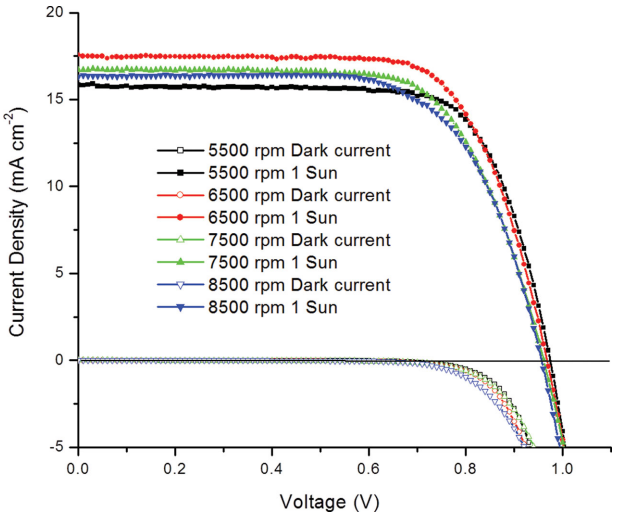

Figure 6. Current–voltage characteristics of $CH_3NH_3PbI_3$ based solar cells obtained while using different spin-speeds for PbI_2 deposition, measured in dark and under illumination.

16.2 mA cm^{-2}, V_{oc} of 1025 mV, and *FF* of 0.69, resulting in a PCE of 11.5% when toluene was used as a solvent (in the HTM solution). Whereas with the same solvent that was used for S197, i.e., chlorobenzene, PTTA showed a J_{sc} of 15.2 mA cm^{-2}, V_{oc} of 953 mV, *FF* of 0.69, and finally a PCE of 10.1%. The statistical data are summarized in Table S5-S6 in the Supporting Information. The high performance in toluene for PTAA is mainly due to the solvent effect. However, due to the solubility limitation, toluene can not be used for S197 as a solvent. From a comparison between S197 and the well-known polymer PTAA, it is apparent that the lower hole mobility of the oligomer (compared to PTAA) can be compensated with the better infiltration/contact with perovskite, which probably enhances the J_{sc}.

In summary, we have developed a novel hole transporting oligomer exhibiting low molecular weight for fabricating efficient $CH_3NH_3PbI_3$ based solar cells. The appropriate molecular size and energy levels, high hole mobility, good solubility, and low cost are essential factors making it to be a promising candidate. We also found that the purity, loading and morphology of the perovskite are very critical parameters for obtaining high efficiency. The oligomer presented here and the overall fabrication method could be a facile and new approach for fabricating efficient perovskite based photovoltaic devices.

Experimental Section

Synthesis of the 2,4-Dimethoxyphenyl Monomer: Tetrakis-(triphenylphosphine)palladium(0) (6.62 g, Peakdale) was added to a mixture of 4-bromo-N,N-bis(4-chlorophenyl)aniline (75 g), 2,4-dimethoxyboronic acid (38.2 g, Alfa-Aesar) and sodium carbonate (64.7 g) in tetrahydrofuran (1120 mL) and H_2O (750 mL) under argon and the mixture was heated to reflux overnight. The organics were separated, the aqueous layer was extracted with ethyl acetate and the combined organics were dried and concentrated to a black solid. The solid was adsorbed onto silica and columned eluting ethyl acetate/heptanes mixtures to give a green/brown solid. Methanol was added and the mixture was stirred for 20 min then filtered and washed with methanol. Methanol was added, the mixture was heated to 40 °C and dichloromethane was added portion wise until all solids had dissolved. The solution was stirred for 10 min, cooled in an ice-bath for 1 h then the solids were filtered, washed with 50:50 methanol/dichloromethane and dried to give the product as a light green/brown solid. Yield: 40.8 g. ^{1}H NMR (400MHz, $CDCl_3$): δ 7.40 (2H, d, ArH), 7.19–7.25 (5H, m, ArH), 7.00–7.05 (6H, m, ArH), 6.55 (2H, m, ArH), 3.84 (3H, s, OMe), 3.81 (3H, s, OMe).

Synthesis of S197: A 500 mL three neck round bottom flask was fitted with overhead stirrer, thermometer, air condenser, Claisen adaptor and septum inlet. The apparatus was flushed with argon. N,N-dimethylacetamide (150 mL, Sigma-Aldrich) was charged and degassed for 15 min. Triphenylphosphine (4.54 g, Sigma-Aldrich), 2,2′-bipyridyl (210 mg, Sigma-Aldrich), zinc (6.71 g, Alfa-Aesar) and nickel (II) chloride (130 mg, Sigma-Aldrich) were added to the vessel and the contents were heated to 70–80 °C where the mixture turned red-brown in color. A few crystals of iodine were added, and the reaction was left to stir for 1 h. The monomer (15 g) was added to the vessel followed by anhydrous toluene (24 mL, Sigma-Aldrich). The reaction was left to stir for 15 h before being cooled to room temperature. Filtered, washing the solids with N,N-dimethylacetamide. The filter cake was dissolved in dichloromethane (500 mL) and filtered through celite. The filtrates were washed with 1 M hydrochloric acid (250 mL), water (250 mL) and 10% brine solution (250 mL), dried (magnesium sulphate) and concentrated to give a yellow solid. This material was dissolved into dichloromethane (500 mL) and filtered through silica, eluting with dichloromethane. Product fractions were combined and concentrated to give a yellow solid. This was dissolved in chloroform (250 mL) and charcoal treated three times (3 × 0.867 g charcoal). The filtrates were then concentrated to give a yellow solid. This material was dissolved in chloroform (150 mL) and added dropwise to a stirred portion of methanol (750 mL). The resulting suspension was stirred for 1 hour before being collected by filtration to give a pale yellow powder. Yield: 6.67 g, M_n = 3368 g mol^{-1}, n = 8.8, polydispersity = 2.4.

Solar Cell Fabrication: CH_3NH_3I was synthesized as reported earlier.[12] PbI_2 was ordered from Sigma-Aldrich and used as received. All the other chemicals were purchased from commercial sources and were used without further purification. The etched fluorine-doped tin oxide (FTO) conductive glass (TEC 7, Pilkington) was cleaned with 2% helmanex aqueous solution, acetone, then ethanol. The compact TiO_2 layer (around 60 nm) was deposited by spray pyrolysis at 450 °C using titanium diisopropoxide bis(acetylacetonate) solution as precursor and O_2 as carrier gas, followed by $TiCl_4$ treatment (20 mM $TiCl_4$ aqueous solution)

Table 1. Photovoltaic parameters derived from *J–V* measurement for the devices based on different spin-speeds of PbI_2 deposition.

PbI_2 spin-speed	Light intensity [mW cm^{-2}]	J_{sc} [mA cm^{-2}]	V_{oc} [mV]	*FF*	*PCE* [%]
5500 rpm Average ± std dev [%]	98.3	15.8 (16.0 ± 0.3)	974 (973 ± 12)	0.73 (0.69 ± 0.03)	11.4 (10.9 ± 0.5)
6500 rpm Average ± std dev [%]	99.6	17.6 (17.4 ± 0.1)	967 (975 ± 5)	0.70 (0.68 ± 0.02)	12.0 (11.6 ± 0.3)
7500 rpm Average ± std dev [%]	99.5	16.7 (16.6 ± 0.2)	960 (963 ± 10)	0.69 (0.67 ± 0.03)	11.1 (10.8 ± 0.3)
8500 rpm Average ± std dev [%]	96.0	16.3 (16.3 ± 0.1)	956 (933 ± 15)	0.68 (0.67 ± 0.02)	11.0 (10.5 ± 0.4)

© 2014 WILEY-VCH Verlag GmbH & Co. KGaA, Weinheim

at 70 °C for 30 min, and sintering at 500 °C for 30 min. The mesoporous TiO_2 film was prepared by spin-coating the TiO_2 (Dyesol 18NRT) paste at 5000 rpm for 30 s, then sintering at 500 °C for 30 min in air. The 1.0 M PbI_2 (in DMF) solution was dropped on the TiO_2 surface, and spin-coated at 5500/6500/7500/8500 rpm for 90 s in the dry air box. The film was then annealed at 70 °C for 15 min. After cooling down to room temperature, the film was dipped into CH_3NH_3I solution (10 mg mL^{-1} in 2-propanol) for 25 s, then dried at 70 °C for another 15 min. The HTM, consisting of 5 mM S197, 1.3 mM LiTFSI, and 0.05 M TBP, in chlorobenzene, was spin-coated on the top of the perovskite layer with the spin speed of 3500 rpm. For PTAA, a HTM solution of 1 mM PTAA, 1.3 mM LiTFSI, 0.05 M TBP in toluene or chlorobenzene, was spin-coated under the same conditions as mentioned before. Finally, 60 nm of Au was deposited by thermal evaporation under a pressure of 5×10^{-6} Torr on the top of the HTM as the back contact.

Photovoltaic Characterization: A 450 W xenon lamp (Oriel) was used as the light source, equipped with a Schott K133 Tempax sunlight filter. The current–voltage characteristics were measured by applying an external potential bias to the device, and recorded the generated photocurrent with a Keithley model 2400 digital source meter. IPCE spectra were measured by an array of white light emitting diodes. The excitation beam (from a 300 W xenon lamp) passed through a Genimi-180 double monochromator (Jobin Yvon Ltd) and chopped at approximately 2 Hz before it illuminated the device. The spectra were recorded using a Model SR830 DSP Lock-In Amplifier. In both cases, the device was measured by using a black mask with an area of 0.285 cm^2.

Supporting Information

Supporting Information is available from the Wiley Online Library or from the author.

Acknowledgements

The authors acknowledge financial contribution from Greatcell Solar SA, Epalinges, Switzerland, the European Community's Seventh Framework Programme (FP7/2007–2013) under grant agreement n° 246124 of the SANS project, the "ORION" grant agreement no. NMP-229036 and "CE-Mesolight" EPFL, the ECR advanced grant agreement no. 247404 and the King Abdullah University of Science and Technology (KAUST, Award n° KUS-C1–015–21). MKN thanks the Global Research Laboratory (GRL) Program, Korea, and World Class University programs (Photovoltaic Materials, Department of Material Chemistry, Korea University) funded by the Ministry of Education, Science and Technology through the National Research Foundation of Korea (No. R31–2008–000–10035–0). M.I.D gratefully acknowledges financial support from the Swiss confederation under the Swiss Government Scholarship programme.

Received: June 13, 2014
Revised: July 26, 2014
Published online:

[1] M. Grätzel, *Acc. Chem. Res.* **2009**, *42*, 1788.
[2] A. Hagfeldt, G. Boschloo, L. Sun, L. Kloo, H. Pettersson, *Chem. Rev.* **2010**, *110*, 6595.
[3] A. Yella, H-W. Lee, H. N. Tsao, C. Yi, A. K. Chandiran, M. K. Nazeeruddin, E. W.-G. Diau, C-Y. Yeh, S. M. Zakeeeruddin, M. Grätzel, *Science* **2011**, *334*, 629.
[4] M. A. Green, K. Emery, Y. Hishikawa, W. Warta, E. D. Dunlop, *Prog. Photovolt. Res. Appl.* **2013**, *21*, 827.
[5] J. Burschka, A. Dualeh, F. Kessler, E. Baranoff, N.-L. Cevey-Ha, C. Yi, M. K. Nazeeruddin, M. Grätzel, *J. Am. Chem. Soc.* **2011**, *133*, 18042.
[6] S. Wang, D. B. Mitzi, C. A. Field, A. Guloy, *J. Am. Chem. Soc.* **1995**, *117*, 5297.
[7] C. R. Kagan, D. B. Mitzi, C. D. Dimitrakopoulos, *Science* **1999**, *286*, 945.
[8] A. Kojima, K. Teshima, Y. Shirai, T. Miyasaka, *J. Am. Chem. Soc.* **2009**, *131*, 6050.
[9] J.-H. Im, C.-R. Lee, J.-W. Lee, S.-W. Park, N.-G. Park, *Nanoscale* **2011**, *3*, 4088.
[10] H.-S. Kim, C.-R. Lee, J.-H. Im, K.-B. Lee, T. Moehl, A. Marchioro, S.-J. Moon, R. Humphry-Baker, J.-H. Yum, J. E. Moser, M. Grätzel, N.-G. Park, *Sci. Rep.* **2012**, *2*, 1.
[11] M. M. Lee, J. Teuscher, T. Miyasaka, T. N. Murakami, H. J. Snaith, *Science* **2012**, *338*, 643.
[12] L. Etgar, P. Gao, Z. Xue, P. Qin, A. K. Chandiran, B. Liu, M. K. Nazeeruddin, M. Grätzel, *J. Am. Chem. Soc.* **2012**, *134*, 17396.
[13] W. A. Laban, L. Etgar, *Energy Environ. Sci.* **2013**, *6*, 3249.
[14] J. Burschka, N. Pellet, S.-J. Moon, R. Humphry-Baker, P. Gao, M. K. Nazeeruddin, M. Grätzel, *Nature* **2013**, *499*, 316.
[15] M. Liu, M. B. Johnston, H. J. Snaith, *Nature* **2013**, *501*, 395.
[16] D. Liu, T. L. Kelly, *Nat. Photonics* **2014**, *8*, 133.
[17] J. M. Ball, M. M. Lee, A. Hey, H. Snaith, *Energ Environ Sci.* **2013**, *6*, 1739.
[18] O. Malinkiewicz, A. Yella, Y.-H. Lee, G. M. Espallargas, M. Grätzel, M. K. Nazeeruddin, H. Bolink, *Nat. Photonics* **2014**, *8*, 128.
[19] S. D. Stranks, G. E. Eperon, G. Grancini, C. Menelaou, M. J. P. Alcocer, T. Leijtens, L. M. Herz, A. Petrozza, H. J. Snaith, *Science* **2013**, *342*, 341.
[20] G. Xing, N. Mathews, S. Sun, S. S. Lim, Y. M. Lam, M. Grätzel, S. Mhaisalkar, T. C. Sum, *Science* **2013**, *342*, 344.
[21] H.-S. Kim, I. Mora-Sero, V. Gonzalez-Pedro, F. Fabregat-Santiago, E. J. Juarez-Perez, N.-G. Park, J. Bisquert, *Nat Commun.* **2013**, *4*, 2242.
[22] P. Qin, A. L. Domanski, A. K. Chandiran, R. Berger, H.-J. Butt, M. I. Dar, T. Moehl, N. Tetreault, P. Gao, S. Ahmad, M. K. Nazeeruddin, M. Grätzel, *Nanoscale.* **2014**, *6*, 1508.
[23] Q. Chen, H. Zhou, Z. Hong, S. Luo, H.-S. Duan, H.-H. Wang, Y. Liu, G. Li, Y. Yang, *J. Am. Chem. Soc.* **2014**, *136*, 622.
[24] J. H. Heo, S. H. Im, J. H. Noh, T. N. Mandal, C.-S. Lim, J. A. Chang, Y. H. Lee, H-J. Kim, A. Sarkar, M. K. Nazeeruddin, M. Grätzel, S. I. Seok, *Nat. Photonics.* **2013**, *7*, 486.
[25] J. H. Noh, S. H. Im, J. H. Heo, T. N. Mandal, S. I. Seok, *Nano Lett.* **2013**, *13*, 1764.
[26] B. Cai, Y. Xing, Z. Yang, W.-H. Zhang, J. Qiu, *Energy Environ. Sci* **2013**, *6*, 1480.
[27] Y. S. Kwon, J. Lim, H.-J. Yun, Y.-H. Kim, T. Park, *Energy Environ. Sci* **2014**, *7*, 1454.
[28] N. J Jeon, J. Lee, J. H. Noh, M. K. Nazeeruddin, M. Grätzel, S. I. Seok, *J. Am. Chem. Soc.* **2013**, *135*, 19087.
[29] J. A. Christians, R. C. M. Fung, P. V. Kamat, *J. Am. Chem. Soc.* **2014**, *136*, 758.
[30] P. Qin, S. Tanaka, S. Ito, N. Tetreault, K. Manabe, H. Nishino, M. K. Nazeeruddin, M. Grätzel, *Nat. Commun.* **2014**, *5*, 3834.
[31] Z. Ning, H. Tian, *Chem. Commun.* **2009**, 5483.

© 2014 WILEY-VCH Verlag GmbH & Co. KGaA, Weinheim